Magnetic phase diagram of the $HoRh_{2-x}Ru_xSi_2$ solid solution

1998 J. Phys.: Condens. Matter 10 6367

(http://iopscience.iop.org/0953-8984/10/28/016)

J. Phys.: Condens. Matter **10** (1998) 6367–6379. Printed in the UK PII: S0953-8984(98)89900-1

Magnetic phase diagram of the $HoRh_{2-x}Ru_xSi_2$ solid solution

S Baran†, M Hofmann‡, J Leciejewicz§, B Penc†, P Starowicz†, N Stüsser‡, A Szytuła†¶ and A Zygmunt‖

† Institute of Physics, Jagellonian University, Reymonta 4, 30-059 Kraków, Poland
‡ BENSC, Hahn–Meitner Institute, Berlin-Wannsee, Germany
§ Institute of Nuclear Chemistry and Technology, Warszawa, Poland
‖ Institute of Low Temperatures and Structural Research, Polish Academy of Sciences, Wrocław, Poland

Received 9 December 1997, in final form 20 April 1998

Abstract. The magnetic phase diagram of the solid solution $HoRh_{2-x}Ru_xSi_2$ ($ThCr_2Si_2$-type crystal structure) has been established based on neutron diffraction data collected for seven intermediate compositions and supplemented by magnetometric data. Collinear antiferromagnetic structures described by the wave vectors $[0, 0, 1]$, $[1/2, 1/2, 1/2]$ and $[1/2, 1/2, 0]$ develop successively as the Ru concentration denoted by the index x rises from 0 to 0.75, followed by antiferromagnetic sine modulated structures with wave vectors $\boldsymbol{k} = [k_x, k_x, k_z]$, $\boldsymbol{k} = [k_x, k_x, 0]$ and $\boldsymbol{k} = [k_x, 0, 0]$ observed in the concentration range $0.5 < x < 2$.

1. Introduction

Investigations of magnetic properties of solid solutions with boundary compounds exhibiting different magnetic ordering schemes provide interesting information on the interplay of competing interactions among magnetic moments in crystals. They manifest themselves by a variety of magnetic structures observed in neutron diffraction experiments performed on transient compositions.

Lanthanide ternary phases with the $ThCr_2Si_2$-type crystal structure are very suitable objects for such studies, since they have a simple structure with a tetragonal unique axis and an advantageous c/a-ratio of about 2–2.5. These properties facilitate considerably the interpretation of neutron diffractograms obtained for polycrystalline samples.

The $ThCr_2Si_2$-type compounds RT_2X_2 show magnetic properties which depend on the nature of all three constituting elements: R—the lanthanide atom, T—the transition metal atom—and X—non-metal atoms like Ge,Si,Sn,P,Sb. Consequently, a large number of various magnetic structures have been determined in the course of neutron diffraction studies [1]. The existence of a solid solution, in which the content of the transition metal element changes continuously, gives the possibility to trace the influence of their electronic structure on the magnetic properties of the system, in particular, on the long range magnetic order in the transient compounds. Good examples are provided by the solid solutions $NdRh_{2-x}Ru_xSi_2$ [2] and $TbRh_{2-x}Ru_xSi_2$ [3]. Neutron diffraction studies have shown that

¶ Corresponding author. E-mail address: szytula@if.uj.edu.pl

0953-8984/98/286367+13$19.50

the incommensurate magnetic structures observed in these systems can be correlated with the number of free electrons donated by the transition metals to the conduction band.

X-ray diffraction data indicate that also the $HoRh_{2-x}Ru_xSi_2$ solid solution is formed over the whole composition range denoted by the index $0 \leqslant x \leqslant 2$. As one may expect, the magnetic properties of transient compounds have been found to depend on the transition metal content x [4]. The boundary compounds of this system exhibit different magnetic structures: $HoRh_2Si_2$ was found to be a collinear antiferromagnet characterized by the wave vector $\boldsymbol{k} = [0, 0, 1]$ with $T_N = 27$ K [5] while $HoRu_2Si_2$ shows a modulated antiferromagnetic order with $\boldsymbol{k} = [0.22, 0, 0]$ below $T_N = 19$ K [6]. The magnetic moment direction in $HoRh_2Si_2$ was found to make the angle of $28 \pm 3^\circ$ with the c-axis below $T_t = 11$ K and is parallel to the c-axis above T_t. This magnetic structure is usually denoted as AFI. In $HoRu_2Si_2$ the magnetic moment is parallel to the c-axis.

A neutron diffraction study has been therefore undertaken, supplemented by earlier [4] and new magnetometric measurements. In total, seven transient compounds of the $HoRh_{2-x}Ru_xSi_2$ system were synthesized and investigated: $x = 0.25$, 0.50, 0.75, 1.00, 1.25, 1.50, 1.75. A part of the data has been reported during the *12th International Conference on Solid Compounds of Transition Elements* in Saint-Malo 1997 and published in [7].

2. Experiment

The measurements were carried out on polycrystalline samples which were single phases with $ThCr_2Si_2$-type crystal structure. Prolonged annealing times were adopted to ensure the homogeneity of the samples. Details of preparation procedures and x-ray diffraction tests are reported in [4].

Neutron diffractograms were recorded using the E6 instrument at the reactor BER II in the Berlin Neutron Scattering Centre, Hahn–Meitner Institut. The neutron wavelength was 2.38(2) Å. Data processing was carried out using the FULLPROF program [8] with neutron scattering lengths values taken from [9] and magnetic form factor for the Ho^{3+} ion from [10]. Mean neutron scattering lengths for $(2-x)\mathrm{Rh} + x\mathrm{Ru}$ nuclei distributed at random in the 4(d) site were also varied in the data processing controlling the experimental value of the index x. Tables of observed and calculated neutron intensities for all structures reported in this paper are obtainable on request from the corresponding author.

The samples were additionally controlled by ac and dc magnetic susceptibility and magnetization measurements performed using a mutual inductance method, a SQUID magnetometer and a vibrating magnetometer.

3. Results

3.1. Crystal structure

Neutron diffractograms obtained above the respective magnetic ordering temperatures confirmed that all samples exhibit the $ThCr_2Si_2$-type structure, space group $I4/mmm$, with atoms in the following sites:

Ho in 2(a):	$0, 0, 0$;	$1/2, 1/2, 1/2$;		
Rh and Ru distributed at random in 4(d):				
	$0, 1/2, 1/4$;	$1/2, 0, 3/4$;	$1/2, 0, 1/4$;	$0, 1/2, 3/4$;
Si in 4(e):	$0, 0, z$;	$0, 0, \bar{z}$;	$1/2, 1/2, 1/2 + z$;	$1/2, 1/2, 1/2 - z$.

The lattice parameter, unit cell volume and c/a-ratio dependences on the composition of the sample derived from low temperature neutron diffraction data do not differ from those obtained from x-ray diffraction measurements performed at room temperature [4] (see table 1). The a lattice parameter and unit cell volume V increase, whereas the c lattice parameter and a/c-ratio decrease with the rise of the concentration index x. The z-parameter increases up to $x = 1.25$ and then decreases with the rise of ruthenium concentration. Since atomic radii of Rh and Ru atoms are almost equal (1.34 Å) [11], the above dependence suggests a change of the chemical bonding character as the concentration of ruthenium rises.

Table 1. Crystal data for $HoRh_{2-x}Ru_xSi_2$ compounds at $T = 1.6$ K.

x	a (Å)	c (Å)	c/a	V (Å^3)	z
0.25	4.0355(6)	9.8643(28)	2.4444(10)	160.64(8)	0.3720(10)
0.5	4.032(5)	9.7213(37)	2.4109(12)	158.06(10)	0.3740(10)
0.75	4.0682(8)	9.7194(30)	2.3891(12)	160.86(9)	0.3737(9)
1.0	4.0829(5)	9.6630(22)	2.3667(8)	161.01(7)	0.3742(13)
1.25	4.0976(7)	9.6332(29)	2.3509(11)	161.74(11)	0.3795(18)
1.5	4.0957(12)	9.5510(37)	2.3319(16)	160.22(15)	0.3775(24)
1.75	4.1374(5)	9.5673(26)	2.3120(10)	163.77(7)	0.3702(10)

3.2. Magnetic data

Figure 1 displays the temperature dependence of the magnetization for some $HoRh_{2-x}Ru_xSi_2$ compounds in the magnetic fields of 50 and 100 Oe. At low temperatures maxima typical for transitions from antiferro- to paramagnetic states are observed. The values of the Néel temperatures corresponding to these maxima are listed in table 2. An additional phase transition to ferromagnetic phase at $T_C = 7.7$ K was observed below $T_N = 9.8$ K for the compound with $x = 1.5$. The reciprocal susceptibility curves recorded for all compounds indicate that above the ordering temperatures, the Curie–Weiss law is obeyed with positive (except for $x = 0.25$) values of the paramagnetic Curie temperatures and almost the same values of the effective magnetic moments on the Ho^{3+} ion (10.61 μ_B). Magnetic parameters including those reported in [4] are collected in table 2.

Table 2. Magnetic data for $HoRh_{2-x}Ru_xSi_2$ compounds.

x	T_N (K)	T_t (K)	θ_p (K)	μ_{eff} (μ_B)	μ_S^{a} (μ_B)	H_{cr}^{b} (kOe)
0	27	11	+8	10.2	5.5	15, 43.2
0.25	19	8.4	−6.2	10.33	6.5	11, 31
0.5	4		+1	10.1	6.2	—
0.75	4.6		+3	10.0	5.8	—
1.0	5.5		+5.0	10.5	6.5	—
1.25	5.7		+6	10.0	6.0	—
1.5	9.8	7.7	+21	10.0	6.5	—
1.75	16.4		+5.9	10.4	6.6	1.6
2.0	19		+11.6	10.6	6.8	4.5

[a] At $T = 4.2$ K and $H = 50$ kOe.
[b] At $T = 4.2$ K.

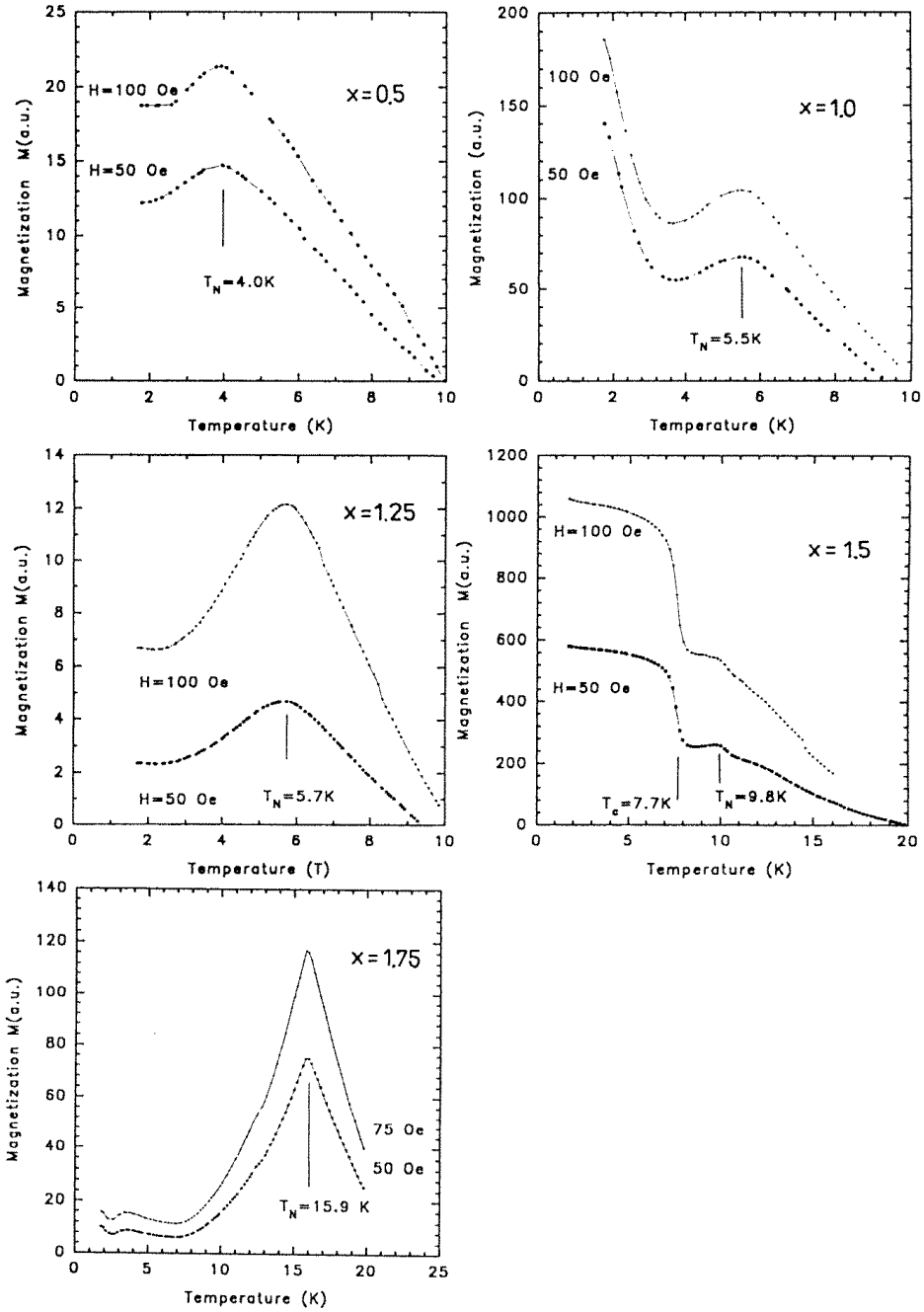

Figure 1. Magnetization–temperature curves of $HoRh_{2-x}Ru_xSi_2$ for $x = 0.5$, 1.0, 1.25, 1.5 and 1.75 at magnetic fields 50 and 100 Oe.

Magnetization curves recorded at 4.2 K as a function of the external magnetic fields up to 5 T are shown in figure 2. Metamagnetic field-induced transitions have been observed for

the samples with $x = 0$, 0.25, 1.75 and 2.0. For the first two samples, two distinct critical fields are observed. The values of the critical fields decrease with the increase of the Ru content. For $x = 1.75$ and 2.0 only one critical field has been detected. The magnetization of the samples with x between 0.5 and 1.5 rises slowly with increasing magnetic field and saturates above 50 kOe. The obtained values of the magnetic moments (see table 2) are smaller that the free Ho^{3+} ion value (10 μ_B). The change of the field dependence of the magnetization curves indicates that the magnetic properties of title compositions clearly depend on the ruthenium concentration expressed by the index x.

3.3. Magnetic structure

Diffraction peaks of magnetic origin were observed on all neutron patterns recorded at low temperatures below the Néel temperatures. The analysis of their positions and intensities revealed the presence of a number of magnetic ordering schemes appearing successively as ruthenium content was increased.

The diffractogram of $HoRh_{1.75}Ru_{0.25}Si_2$ recorded at 1.6 K shows two groups of magnetic peaks (see figure 3(a)). The first originates from the AFI-type antiferromagnetic structure with the magnetic moment localized on the Ho^{3+} ion making the angle ϕ of $(25 \pm 2)^\circ$. with the tetragonal axis. The second group was indexed on a magnetic unit cell doubled in three directions with the propagation vector $\boldsymbol{k}_1 = [1/2, 1/2, 1/2]$, indicating also antiferromagnetic order with the moments inclined to the tetragonal axis by the angle ϕ of $(9 \pm 2)^\circ$. This structure vanishes at 8.5 K while the AFI-type ordering remains up to 20 K, however, above 8 K, with the ϕ angle equal to zero. At 5 K a new antiferromagnetic structure is formed, characterized by the propagation vector $\boldsymbol{k}_2 = [1/2, 1/2, 0]$. It vanishes at 28 K—the Néel point of $HoRh_{1.75}Ru_{0.25}Si_2$. Figure 3(b) shows the temperature variation of the integral intensities of magnetic peaks characteristic for each magnetic phase detected in this composition and illustrates clearly how different magnetic structures appear and vanish as the temperature rises to the Néel point.

The magnetic peaks observed in the temperature range 1.6–6.5 K in the neutron diffraction patterns of $HoRh_{1.5}Ru_{0.5}Si_2$ compound correspond to the antiferromagnetic structure with $\boldsymbol{k} = [1/2, 1/2, 1/2]$. Neutron diffractograms revealed also that another magnetic phase is present at the temperatures from 1.6 to 3.5 K. This phase was found to exhibit a sine modulated antiferromagnetic structure described by the propagation vector $\boldsymbol{k} = [0.150(1), 0.150(1), 0.473(1)]$. In both above phases the magnetic moment is parallel to the c-axis.

Neutron diffraction patterns of $HoRu_{1.25}Ru_{0.75}Si_2$ show two groups of magnetic peaks below the Néel point at 4.8 K: the first is due to the collinear antiferromagnetic structure with $\boldsymbol{k} = [1/2, 1/2, 1/2]$; the second originates from a sine modulated antiferromagnetic order described by two wave vectors: $\boldsymbol{k}_1 = [0.1418(5), 0.1481(5), 0.3645(25)]$ and $\boldsymbol{k}_2 = [0.1484(5), 0.1484(5), 0.4444(26)]$. The intensity of the $(000^{\pm})$ magnetic reflection plotted against temperature gives the Néel point at 4.8 K.

Neutron diffractograms of $HoRhRuSi_2$ run in the temperature range from 1.6 to 6 K are displayed in figure 4. The observed magnetic peaks were ascribed to a sine modulated antiferromagnetic structure characterized by a pair of wave vectors: $\boldsymbol{k}_1 = [0.1314(5), 0.1314(5), 0.2852(16)]$ and $\boldsymbol{k}_2 = [0.1375(6), 0.1375(6), 0.3130(31)]$. The temperature dependence of the $000^{\pm}$ peak intensity gives the Néel temperature at 5.2 K (see the inset in figure 4).

Neutron diffractograms of $HoRh_{0.75}Ru_{1.25}Si_2$ taken at low temperatures are similar to those obtained for the compound with $x = 1.00$. A sine modulated antiferromagnetic order

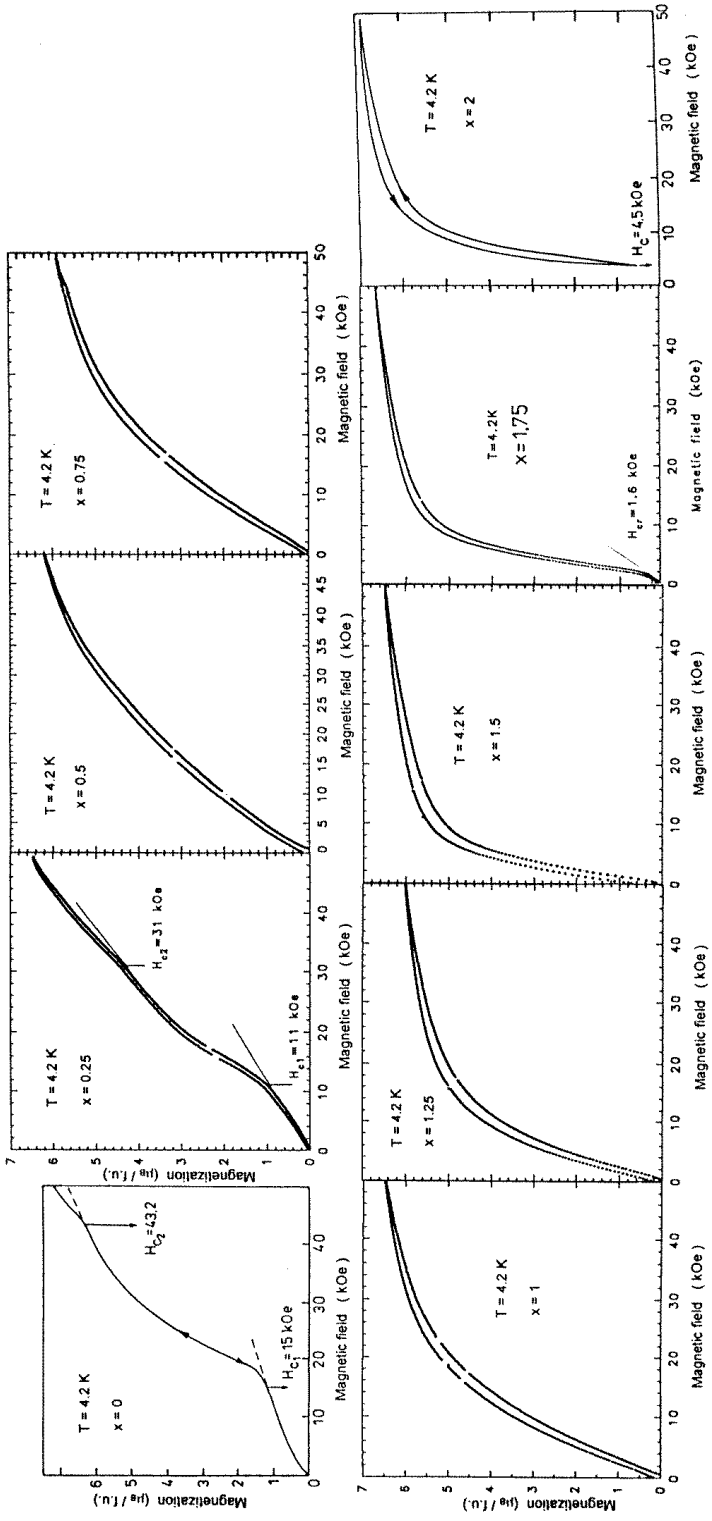

Figure 2. $HoRh_{2-x}Ru_xSi_2$: magnetization at 4.2 K as a function of the applied magnetic fields for different compositions.

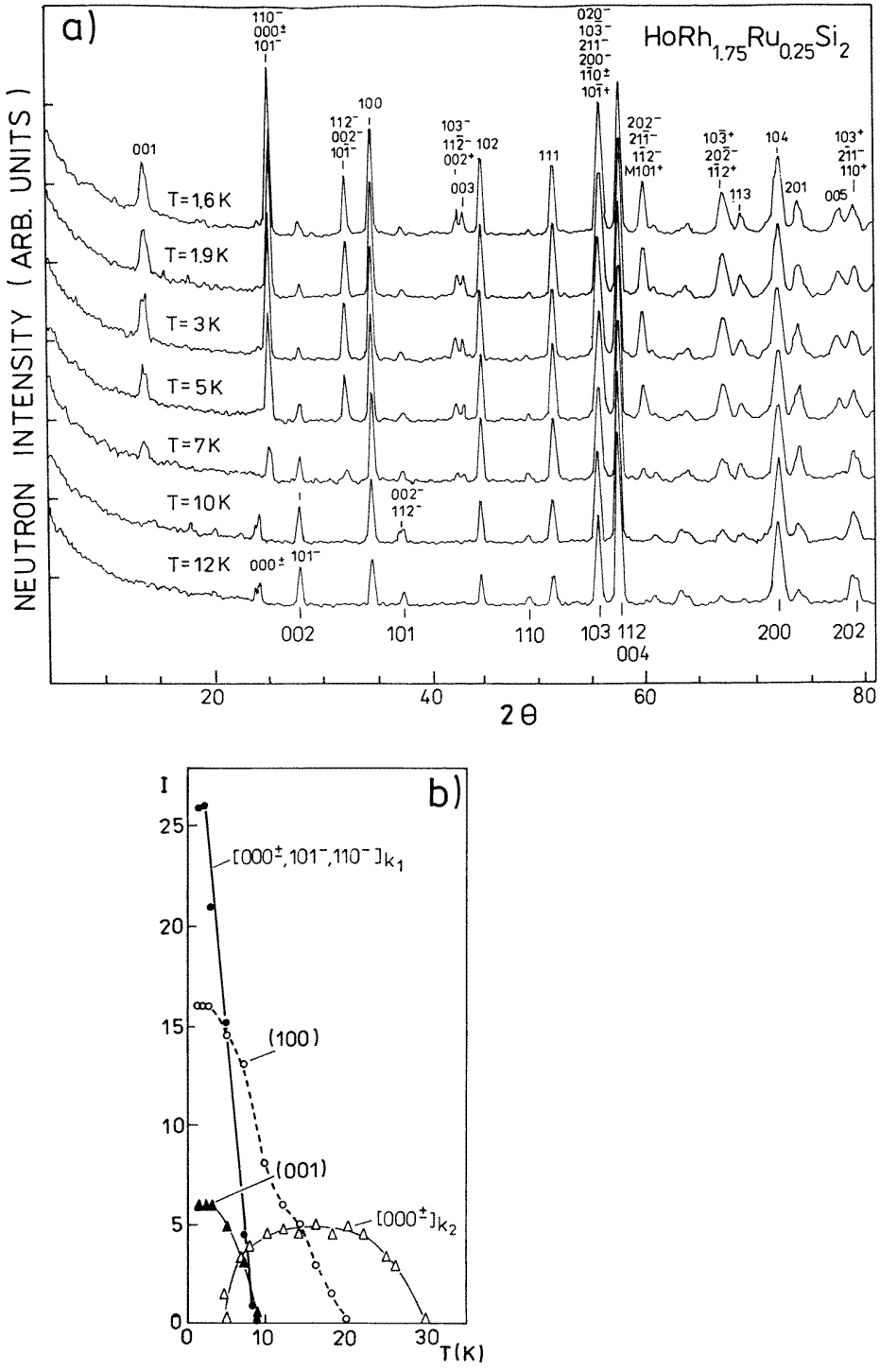

Figure 3. (a) Neutron diffractograms of $HoRh_{1.75}Ru_{0.25}Si_2$ recorded at the temperatures between 1.6 and 12 K. (b) The variation with temperature of magnetic peaks intensities characteristic for the commensurate antiferromagnetic phases observed in $HoRh_{1.75}Ru_{0.25}Si_2$ (see text).

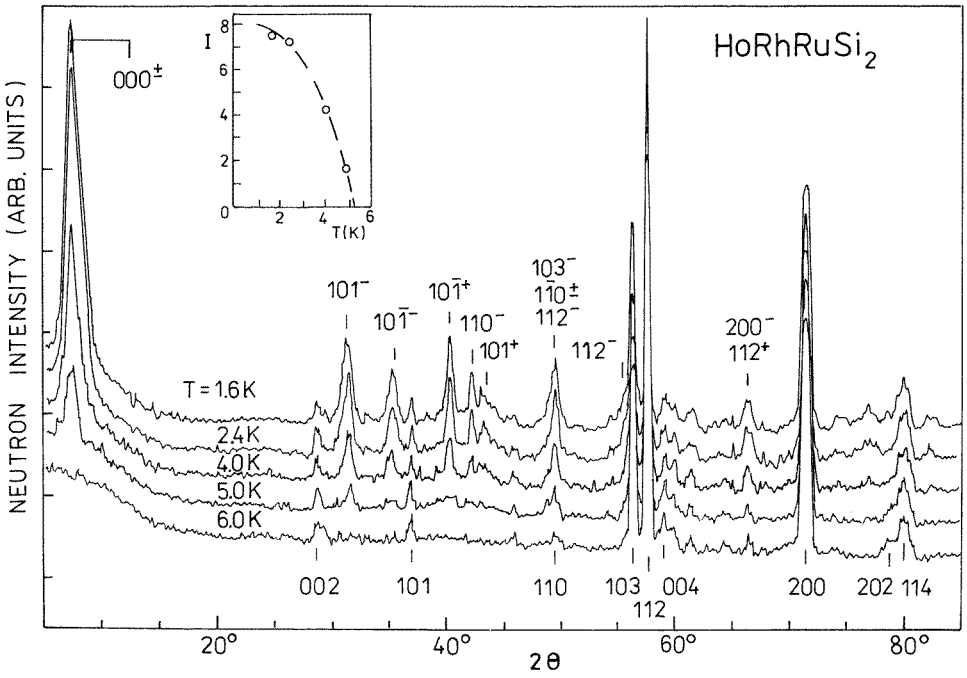

Figure 4. Neutron diffractograms of $HoRh_{1.00}Ru_{1.00}Si_2$ obtained at temperatures between 1.6 and 6 K. The inset show the intensity of the $000^{\pm}$ magnetic peak plotted against temperature.

described also by a pair of wave vectors, $\boldsymbol{k}_1 = [0.1286(3), 0.1286(3), 0.2250(18)]$ and $\boldsymbol{k}_2 = [0.1375(6), 0.1375(6), 0.3130(31)]$ was detected. The change of $000^{\pm}$ magnetic peak intensity with temperature yields the Néel point at 5.8 K.

Figure 5 shows the neutron diffraction patterns of $HoRh_{1.5}Ru_{0.5}Si_2$ measured at different temperatures between 1.5 and 15 K. In the pattern recorded at 1.5 K, an increase of the intensities of the peaks with $h + k + l = 2n$ is observed. This result suggests that the Ho magnetic moment forms a collinear ferromagnetic structure with moments aligned along the tetragonal axis. The ferromagnetic order transforms at 7 K into two sine modulated antiferromagnetic structures characterized by the wave vectors $\boldsymbol{k}_1 = [0.1470(2), 0.1470(2), 0]$ and $\boldsymbol{k}_2 = [0.2851(3), 0, 0]$ which coexist up to the Néel point at 12 K. This follows from neutron diffractograms recorded in the temperature range from 1.5 to 15 K which are shown in figure 5. The stability ranges of the magnetic phases are displayed in figure 6 in which the intensities of magnetic peaks characteristic for each phase are plotted against the temperature. The sine modulated phase with propagation vector $\boldsymbol{k}_1$ is denoted as SM1, that with $\boldsymbol{k}_2$ as SM2. Schematic representation of each structure is shown in figure 7.

Neutron diffractograms of $HoRh_{0.25}Ru_{1.75}Si_2$ were recorded in the temperatures between 1.6 and 17 K. Only one sine modulated antiferromagentic phase has been found. It is described by the wave vector $\boldsymbol{k} = [0.2519(1), 0, 0]$. The Néel point is at 15.5 K.

The determined parameters of all magnetic structures observed in the $HoRh_{2-x}Ru_xSi_2$ system are collected in table 3. The magnetic phase diagram based on neutron diffraction data is shown in figure 8.

Table 3. Magnetic structure parameters for HoRh$_{2-x}$Ru$_x$Si$_2$ compounds determined from neutron diffraction data.

			Low temperature phase				High temperature phase			
x	T_N (K)	T_t (K)	T (K)	k-vector	μ (μ_B)	$\phi\theta$ (°)	T (K)	k-vector	μ (μ_B)	$\phi\theta$ (°)
0[a]	27	11	4.2	0, 0, 1	8.8(2)	28(3)				
0.25	28	8.5	1.6	0, 0, 1	5.94(10)	25.6(1.4)	11	0, 0, 1	4.83(4)	0
				1/2, 1/2, 1/2	5.64(9)	9.0(24)	11	1/2, 1/2, 0	2.45(6)	0
0.5	6.5	3.5	1.6	1/2, 1/2, 1/2	5.10(7)	0	4.0	1/2, 1/2, 1/2	4.1(1)	0
				0.1504(4), 0.1504(4), 0.4728(28)	4.5(9)	0				
0.75	4.8	—	1.6	1/2, 1/2, 1/2	2.40(8)	0				
				0.1449(5), 0.1449(5), 0.3645(25)	6.43(17)	0				
				0.1484(5), 0.1484(5), 0.4444(26)	6.16(17)	0				
1.0	5.2	—	1.6	0.1314(5), 0.1314(5), 0.2852(16)	7.15(8)	0				
				0.1410(8), 0.1410(8), 0.3780(44)	4.17(14)					
1.25	5.8	—	1.6	0.1286(3), 0.1286(3), 0.2250(18)	8.22(13)	0				
				0.1375(6), 0.1375(6), 0.3130(31)	6.13(17)	0				
1.5	12	7	1.6	0, 0, 0	8.32(20)	0	8	0.1470(2), 0.1470(2), 0	6.00(10)	0
								0.285(3), 0, 0	5.66(11)	0
							10	0.2869(3), 0, 0	5.64(9)	0
1.75	15.5	—	1.6	0.2519(1),0,0	9.67(14)	0				
2.0[b]	19	—	4.2	0.22,0,0	9.25(5)	0				

ϕ—the angle between the moment direction and the tetragonal c-axis.

[a] Data from [5].

[b] Data from [6].

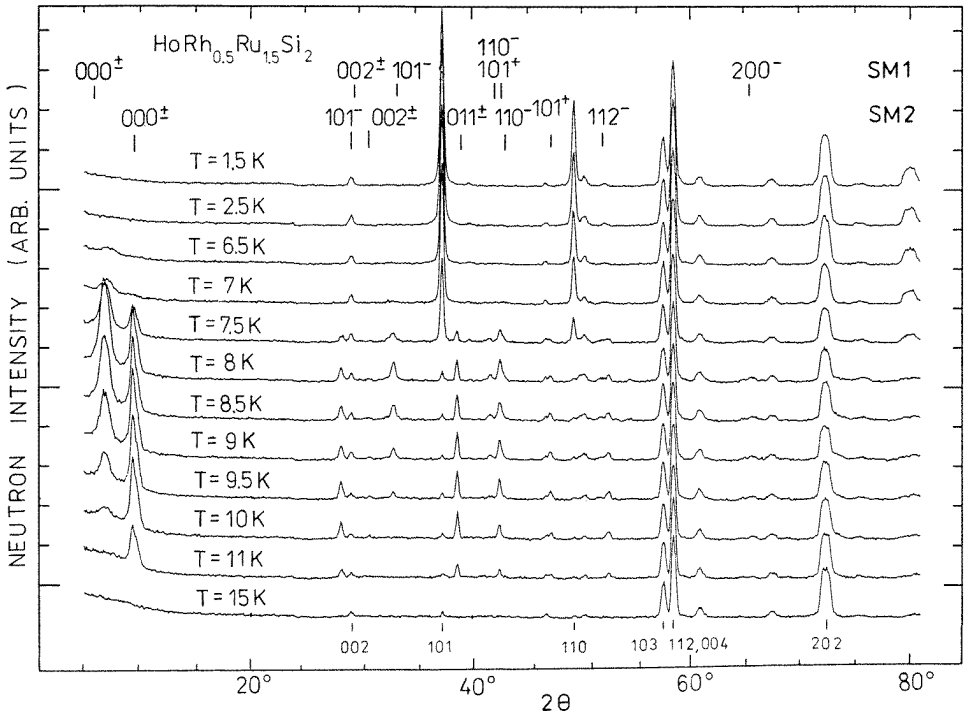

Figure 5. Neutron diffractograms of $HoRh_{1.50}Ru_{0.50}Si_2$ recorded at temperatures between 1.5 and 15 K.

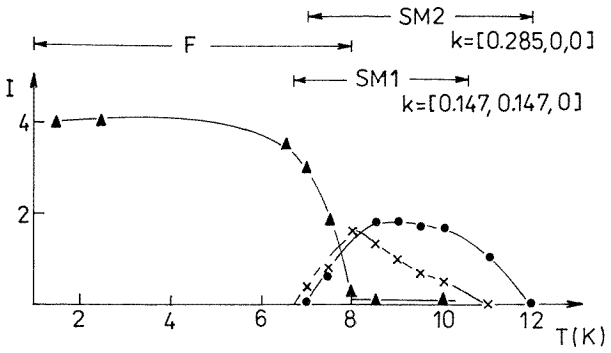

Figure 6. The variation with temperature of magnetic peaks characteristic for each magnetic phase observed in $HoRh_{0.5}Ru_{1.5}Si_2$. F—ferromagnetic structure, SM1 and SM2—antiferromagnetic sine modulated structures.

4. Discussion

All components of the title solid solution crystallize in the $ThCr_2Si_2$-type structure with rhodium and ruthenium distributed at random in the 4(d) site. The results of neutron diffraction measurements supplemented by magnetization data clearly indicate that the magnetic properties of the constituent compounds of this solid solution depend on their

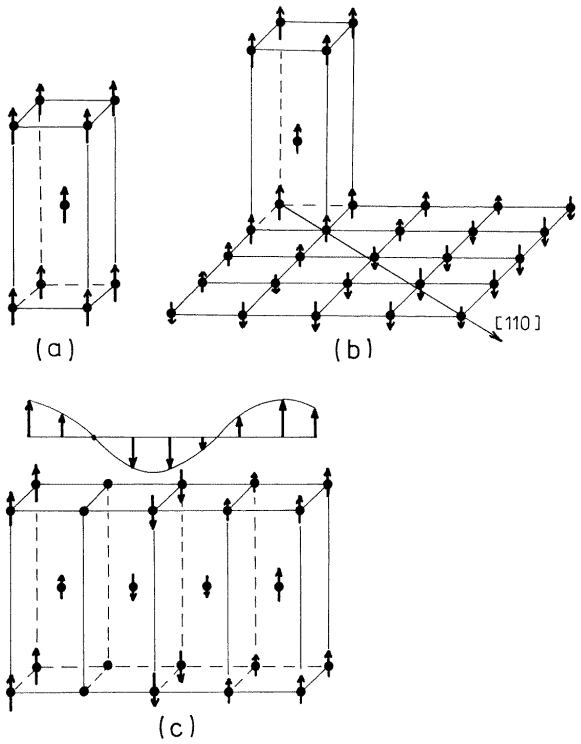

Figure 7. Magnetic structures of $HoRh_{0.5}Ru_{1.5}Si_2$: (a) ferromagnetic; (b) antiferromagnetic sine modulated SM1; (c) antiferromagnetic sine modulated SM2.

chemical composition i.e. relative content of Rh and Ru represented by the index x. Some general trends may be noticed from the magnetic phase diagram shown in figure 8. Collinear antiferromagnetic structures represented by the wave vectors $[0, 0, 1]$, $[1/2, 1/2, 1/2]$ and $[1/2, 1/2, 0]$ operate in the samples containing larger amounts of rhodium. The $[1/2, 1/2, 1/2]$ magnetic structure is still present in the $HoRu_{1.25}Ru_{0.75}Si_2$ compound; however, it coexists already with an antiferromagnetic sine modulated order in the compound with $x = 0.50$. Only antiferromagnetic sine modulated structures are observed in the samples with $x > 1.5$. The k_x and k_y components of their wave vectors only slightly change with the composition index x. On the other hand, the k_z components fall to zero in the compounds with $x = 1.50$, 1.75 and 2.00. These results indicate clearly that the rise of Ru concentration affects the range of magnetic interactions: they remain approximately constant in the basal plane extending over 3.5 to 4.5 a but are reduced from 2 c to 1 c along the tetragonal axis (a, c—the lattice parameters). This behaviour is rather surprising in the compounds crystallizing in the tetragonal system, with fairly large c/a-ratio for which one expects strong uniaxial anisotropy. The possible explanation is given in [12] in terms of a flat dependence of the Fourier transform of the exchange coupling $\boldsymbol{J}(\boldsymbol{k})$ in the $\boldsymbol{k}$-vector space with extrema in the main symmetry directions. Magnetic ordering schemes with different wave vector components may be stable and could be observed in experiment.

The development of incommensurate antiferromagnetic structures with the rise of ruthenium concentration has been also found in the $CeRh_{2-x}Ru_xSi_2$ [13], $NdRh_{2-x}Ru_xSi_2$ [2] and $TbRh_{2-x}Ru_xSi_2$ [3] solid solutions. This regularity probably appears as a result

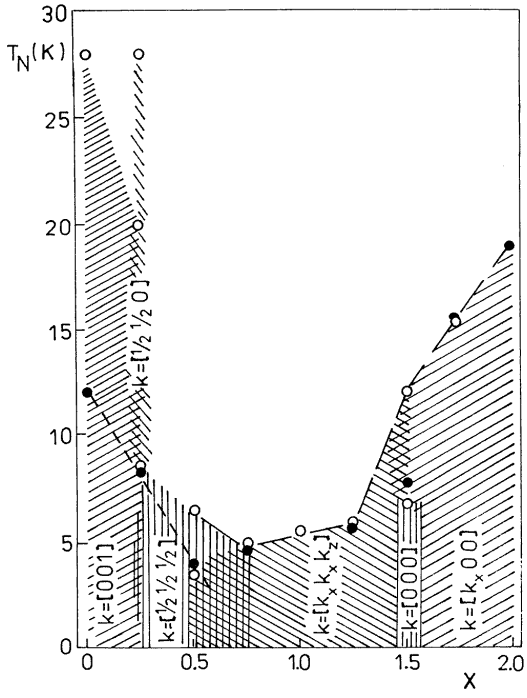

Figure 8. Magnetic phase diagram of the $HoRh_{2-x}Ru_xSi_2$ system based on neutron diffraction and magnetic data.

of density of states changes at the Fermi surface, brought about during the formation of the conduction band by 4d electrons. This effect, in turn, affects the range of magnetic interactions and leads to the modifications in magnetic order observed in experiment. Fairly large Ho^{3+}–Ho^{3+} interionic distances of 4–5 Å and the oscillatory character of the magnetic structures suggest that the magnetic interactions operating in the above solid solutions can be discussed in terms of the RKKY model.

The data collected in table 2 show that starting from $HoRh_{1.5}Ru_{0.5}Si_2$ the magnetic moments on the Ho^{3+} ions are aligned along the tetragonal axis indicating strong Ising-type anisotropy independent on Ru concentration. It is known that the B_2^0-parameter in the crystal electric field (CEF) Hamiltonian for the $4/mmm$ point symmetry plays the dominant role [1]. B_2^0 sign and magnitude have been determined for $HoRh_2Si_2$ [14] and $HoRu_2Si_2$ [15]. In the latter compound the Ho^{3+} magnetic moment is parallel to the tetragonal axis, but in the former it makes the angle of 28(3)° [5]. This angle is a function of the B_2^0/B_4^0-ratio and is given by the formula [16]:

$$\cos\phi = \frac{1}{J}\sqrt{\frac{3}{7}J(J+1) - \frac{3}{70}\left(\frac{B_2^0}{B_4^0}\right)}.$$

The magnitudes of B_2^0 and B_4^0 for $HoRh_2Si_2$ were reported in [14] and the calculation of ϕ gives 36° as compared to 28(3)° found in experiment. The above results indicate that the CEF is the other factor which exercises strong influence on the magnetic properties of the title solid solution.

Acknowledgments

The kind hospitality and financial support granted by the Hahn–Meitner Institute to perform neutron experiments is gratefully acknowledged by four of the authors (SB, JL, PB and AS).

This work has been supported by the European Commission through the PECO 93 Action (contract: ERB PD CT 94 00 88) and the State Committee for Scientific Research in Poland with grant No 2P03B 08708.

References

[1] Szytuła A and Leciejewicz J 1989 *Handbook on the Physics and Chemistry of Rare Earths* vol 12, ed K A Gschneidner Jr and L Eyring (Amsterdam: North-Holland) ch 83, p 139
[2] Jaworska T, Szytuła A, Ptasiewicz-Bąk H and Leciejewicz J 1988 *Solid State Commun.* **65** 261
[3] Jaworska T, Szytuła A, Leciejewicz J and Ptasiewicz-Bąk H 1989 *J. Magn. Magn. Mater.* **82** 313
[4] Ivanov V, Jaworska T, Vinokurova L, Mydlarz T and Szytuła A 1996 *J. Alloys Compounds* **234** 235
[5] Ślaski M, Leciejewicz J and Szytuła A 1983 *J. Magn. Magn. Mater.* **39** 268
[6] Ślaski M, Szytuła A, Leciejewicz J and Zygmunt A 1984 *J. Magn. Magn. Mater.* **46** 114
[7] Baran S, Leciejewicz J, Stüsser N, Ding Y and Szytuła A 1997 *J. Alloys Compounds* **262–263** 225
[8] Rodriguez-Carvajal J 1993 *Physica* B **192** 55
[9] Sears V F 1992 *Neutron News* **3** 26
[10] Freeman A J and Desclaux J D 1979 *J. Magn. Magn. Mater.* **12** 11
[11] Vainshtein B K, Fridkin V M and Indenbom V L 1982 *Modern Crystallography II* (Heidelberg: Springer) p 70
[12] Ball A R, Gignoux D, Schmitt D and Zhang F Y 1995 *J. Magn. Magn. Mater.* **140–6** 1121
[13] Lloret B, Chevalier B, Buffat B, Ettourneau J, Quezel S, Lambarran A, Rossat-Mignod J, Calemczuk R and Bonjour E 1987 *J. Magn. Magn. Mater.* **63/64** 85
[14] Takano Y, Ohhata K and Sekizawa K 1987 *J. Magn. Magn. Mater.* **66** 187
Takano Y, Ohhata K and Sekizawa K 1987 *J. Magn. Magn. Mater.* **70** 242
[15] Łątka K 1989 *Report Institute of Nuclear Physics, Cracow* 1443/PS
[16] Żołnierek Z and Mulak J 1995 *J. Magn. Magn. Mater.* **140–144** 1393